# Beam Charge Measurement for the g2p/GEp experiments

Pengjia Zhu

February 27, 2016

**Abstract**

The g2p/GEp experiments used a solid $NH_3$ polarized target, where the target's polarization is sensitive to temperature and radiation. The beam current was limited to 5-100nA during the experiment to avoid too much depolarization of target. This technical note summarizes the method to calibrate the beam charge monitors (BCM) for the g2p/GEp experiments, with the devices of tungsten calorimeter, new BCM receiver, and DAQ system.

## 1 Hardware

The BCM system used for the g2p/GEp experiments contains two RF cavities, a BCM receiver with related data-acquisition (DAQ) system, and a tungsten calorimeter for calibration. The Unser monitor was not considered due to noisy signal, and the farady cup in injector was not used for calibration due to considerable leakage current between the Halls. The location of them is shown in Fig. 1.

### 1.1 BCM receiver

Since the original RMS-to-DC converter [1] did not work at low current, a new BCM receiver was designed by John Mosson and his colleagues from the JLab instrumentation group for the purpose of achieving a reasonable signal/noise (S/N) ratio in the beam current environment a range of several nanoampere to several micro-ampere [2]. The design diagram is shown in Fig. 2.

The receiver consists of an analog part and a digital part. The analog part includes the amplifier and the mixer. The multiply mixer converts the ratio frequency (RF) signal to the intermediate frequency (IF) signal. The signal is digitized by a 36 MSPS ADC, and applied by a cascaded-integrator–comb (CIC) filter and an infinite-inpulse-response (IIR) filter (10.4 kHz). The CORDIC system is used to get the amplitude and phase of the digital signal [2]. The 20 bit digital signal is converted back to 0-10V analog signal to match the existing Hall A DAQ system using a 18 bit DAC. A DIV unit is used to intercept the signal from 20 bit to 18 bit by applying an adjustable bit shift. More details can be found in [2].

### 1.2 Data acquisition system

The BCM data from the receiver was connected to the DAQ system as shown in Fig. 3. The voltage signal from receiver was split and sent to the V2F module and the HAPPEX ADC.

#### 1.2.1 Scaler

The V2F converts the voltage signal to the frequency signal in order to connect to the scalers for counting. The SIS380x scaler is the VME implement. It has two modes switched by a jumber on the board: SIS3800 and SIS3801. The SIS3800 scaler counts the charge, clock and trigger signals for each event, and delivers them to the data stream when the event trigger is accepted. The counter data for the SIS3800 is only cleared at the beginning of the run, thus the SIS3800 was used to get the counts for the whole run.

The SIS3801 was used to get the helicity gated information. Fig. 4 shows the T-Settle signal from the helicity control board [3] in injector. The high-level T-Settle (70 $\mu s$) indicates the helicity flips, or has unsure helicity status, while the low-level T-Stable (971.65 $\mu s$) indicates the reliable helicity status. The rising edge

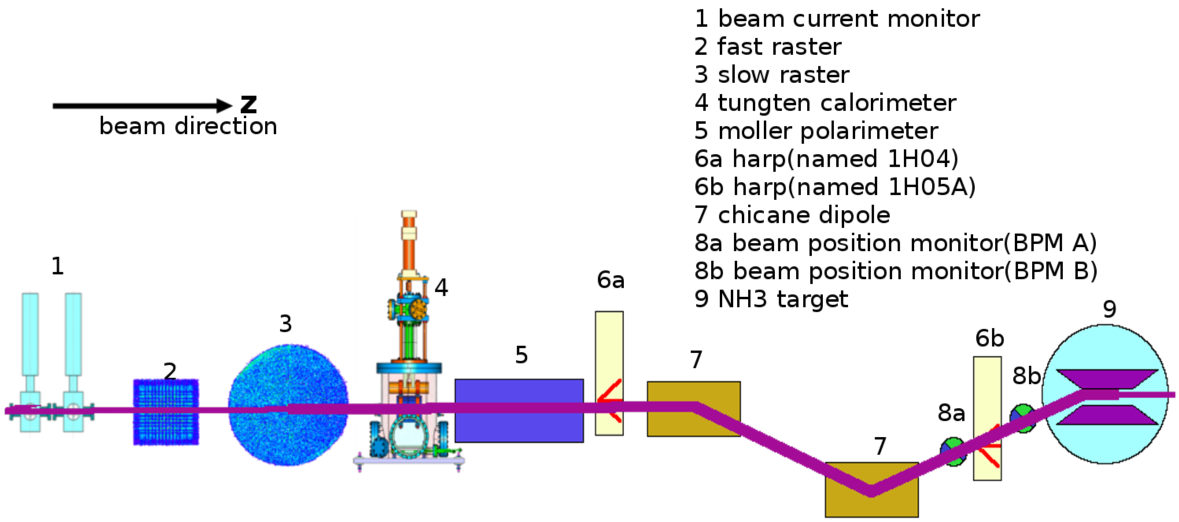


Figure 1: Beamline for the g2p/GEp experiments

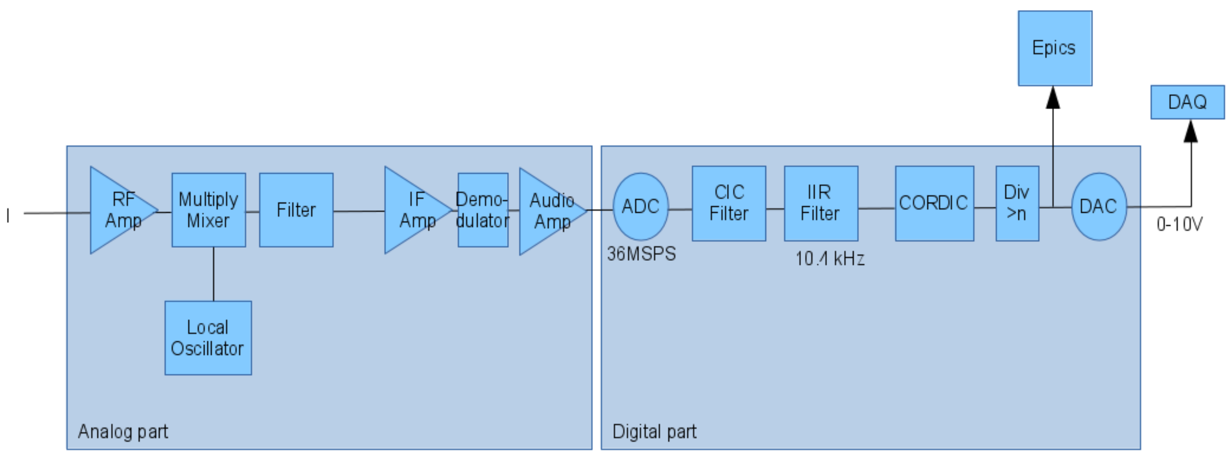


Figure 2: BPM and BCM receiver used for the g2p/GEp experiments

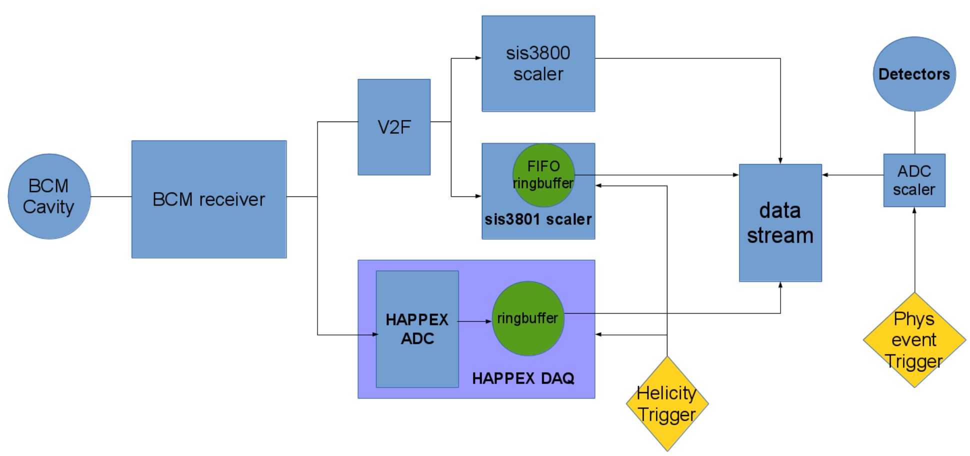


Figure 3: DAQ system for BCM

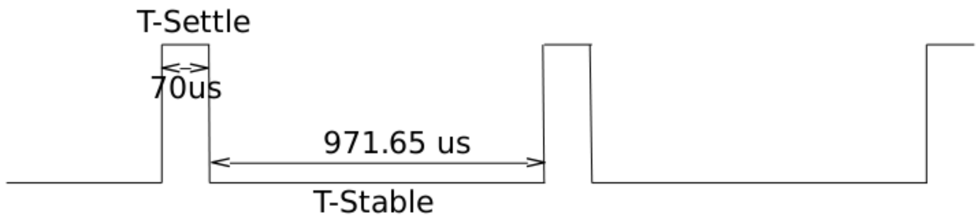


Figure 4: T-Settle signal from helicity control board, with 971.65 $\mu s$ T-Stable time and $70\mu s$ T-Settle time.

of the T-Settle triggers the scaler to save the current counts to the FIFO register, stop the counter and reset the counts. The flipping edge of the T-Settle recovers the counting. The FIFO register is used as a ringbuffer before merging to the standard DAQ system.

### 1.2.2 HAPPEX DAQ

The HAPPEX DAQ uses 18 bit ADCs, which were designed for the parity violation experiments. It has a high bit resolution for measuring small parity violating asymmetries to high precision. This DAQ was reprogrammed and reassembled for the g2p/GEp experiments.

The HAPPEX DAQ contains a timing board (NIM) [4], several 18-bit ADCs [5], a flexible IO (FLEXIO,NIM) [6], a trigger interface module (TI), and a VxWorks CPU. The diagram of HAPPEX DAQ is shown in Fig. 5.

**Timing board** The timing board generates several time signals to control the start and stop integration time of the ADCs. The T-Settle signal was used as the trigger source for the timing board. Based on the trigger signal, the timing board generates a set of signals (Fig. 6). The reset signal controls the ADC integration. The delay time between the baseline signal and the peak signal is used as the integration time, and the digital value difference between them is used as integrated result. The DAC module in the timing board was used as a debugging source during the experiment.

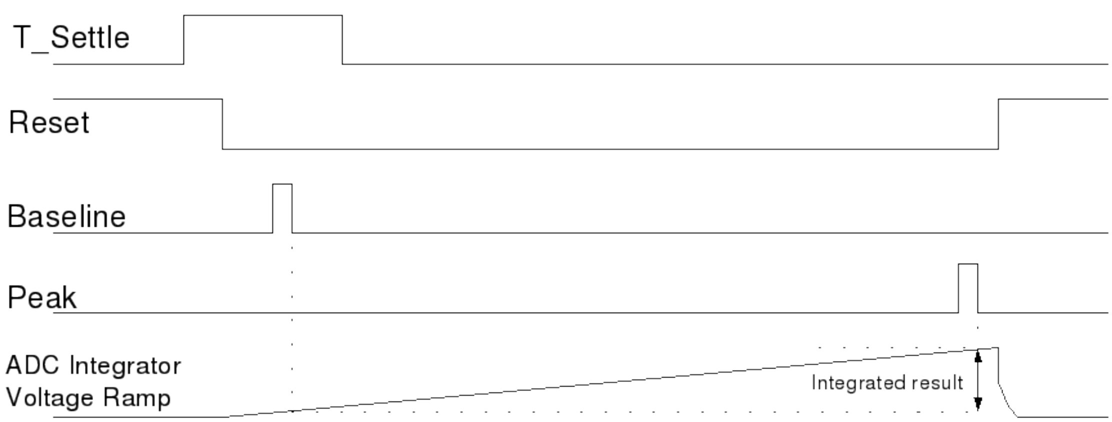


Figure 6: Signals from timing board [6]

**HAPPEX ADC** The HAPPEX ADC was designed for high bit resolution (18 bit) and a small non-linearity ($\leq 2\times10^{-5}$). From the asymmetry measurement test (Fig. 7), the bit resolution for the HAPPEX ADCs were much better than the one for the scalers. The integration time of HAPPEX ADCs controlled by the timing board was 875 $\mu s$, a little bit smaller than the helicity period (1041.65 $\mu s$). The HAPPEX ADCs recorded more precise position and current information than the FASTBUS 1881 ADCs (with an integration time less than 50 $ns$ during the experiment).

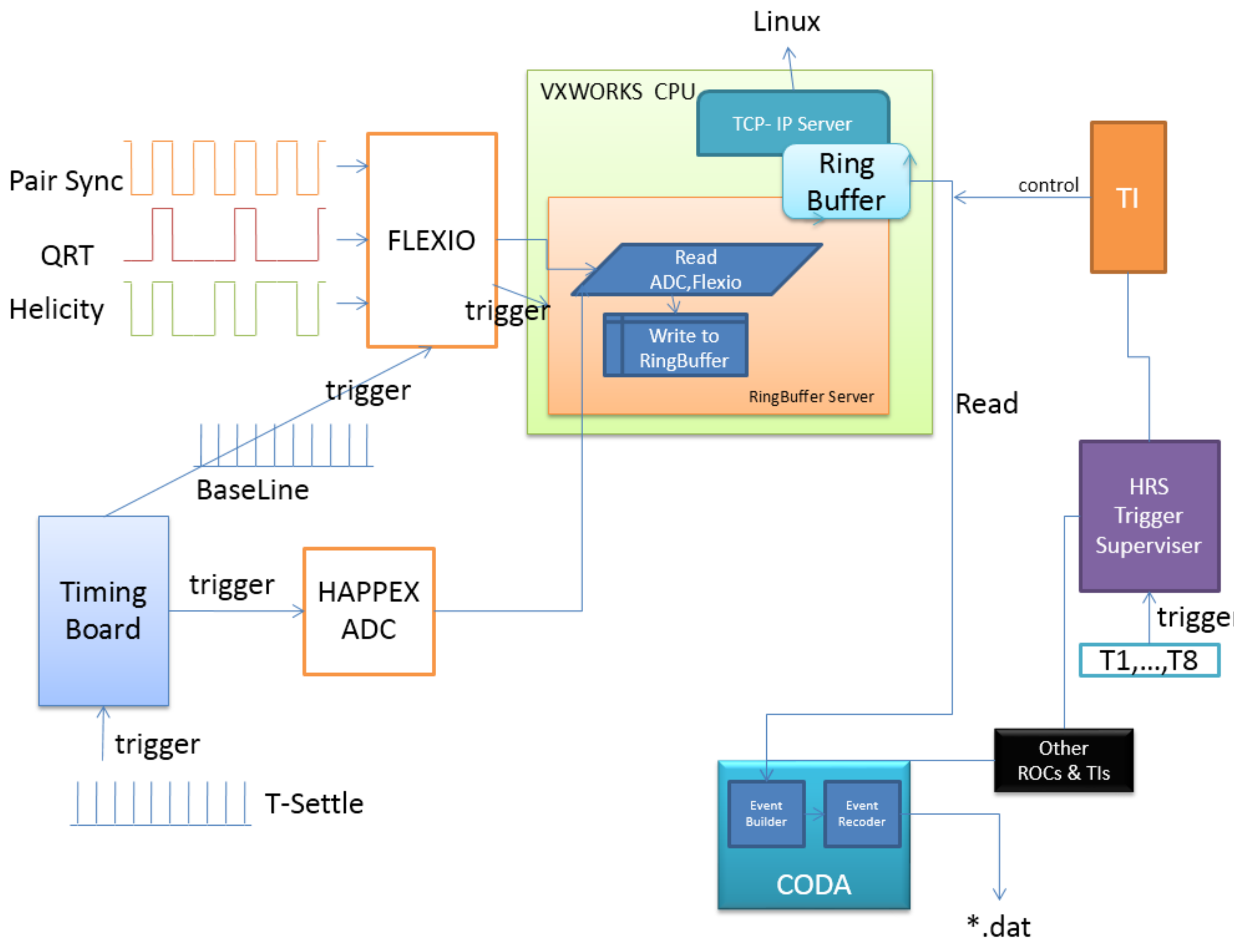


Figure 5: HAPPEX DAQ diagram

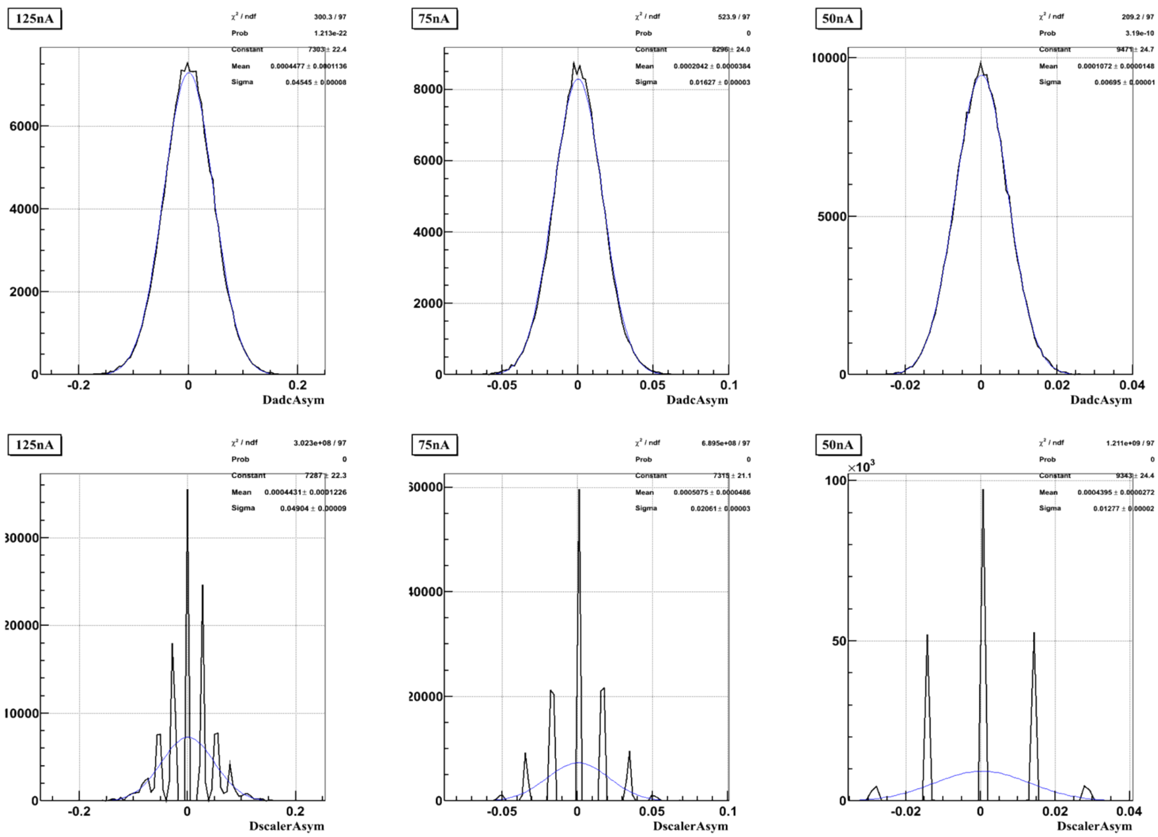


Figure 7: Comparison of charge asymmetry measurements from HAPPEX ADCs and scalers. The top three pictures use HAPPEX ADCs, while the bottom three pictures use scalers. The beam currents from left to right are 125 nA, 75 nA, and 50 nA. The total number of events are same in each histogram.

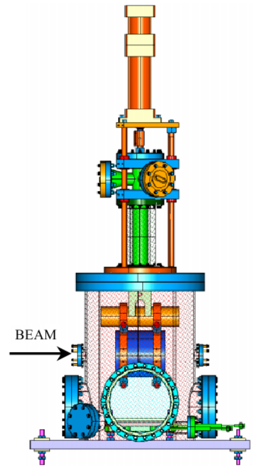


Figure 8: Tungsten Calorimeter

**Flexible IO** The flexible IO is used to record the digital information. The baseline signal peak from the timing board triggers the flexible IO to record the helicity signals. It also provides a trigger signal for the ringbuffer.

**Ring Buffer** A VxWorks CPU controls the data reading from the HAPPEX ADCs and the flexible IO to the ringbuffer server in the CPU's register. For more reliable performance and less CPU occupation, a trigger is used instead of checking the pair sync polarity all of the time. The trigger from the flexible IO has the same period as the T-Settle. Each trigger causes the CPU to read out the data from the flexible IO and the ADCs once. A trigger interface controlled by the HRS trigger superviser reads the data from the ringbuffer server to the data-stream. For the online debugging, a TCP-IP server was running on the CPU to readout the data from the ringbuffer from any Linux computer at any time.

### 1.3 Tungsten Calorimeter

A tungsten calorimeter [7] located downstream of the BCMs and the two rasters [8] for calibrating the BCMs by measuring the beam induced temperature rise, as shown in Fig. 8. The chamber that holds the tungsten is pumped down to vacuum to minimize heat loss. The tungsten is in three positions for the different purpose:

1. Beam charging, the tungsten is in the beam pipe. All of the incoming beam electrons hit the tungsten. The temperature is increasing during this period.
2. Equilibrating, the tungsten moves out of the beam pipe but doesn't touch the cooling plate. The beam turns off. The temperature stabilizes. The measurement of the temperature occurs in this period.
3. Cooling, the tungsten moves to the cooling plate to cool down the tungsten.

For the temperature measurement, six resistance temperature detectors (RTDs) are mounted on the outer surface at each end of the tungsten slug.

## 2 Calibration of the BCMs

Calibration data were taken several times during the experiment. In order to achieve the uniform heat load from the beam over the tungsten surface, the rasters were turned on during the BCM calibration. The limited size of the ringbuffer caused potential loss of data when the read-out speed was lower than the read-in speed. For the deadtime consideration, the DAQ system only read out no more than 50 sets data from the ringbuffer. An additional clock trigger with a frequency larger than 20 Hz ($\geqq$ 960 (helicity frequency) / 50) was added to avoid data loss in the ringbuffer recorded in the data-stream. The clock signal was needed for calculating the pedestal of the scaler and the ADC. For the HAPPEX ADC, the helicity entries was used as the clock.

There were two types of clocks: fast clock and slow clock. The frequency of the fast clock was ∼103.7 KHz, while the frequency of the slow clock was ∼1KHz. The pedestal value is related to the frequency of the clock signal, thus the calibration constants for them are different.

A complete calibration period is shown in Fig. 9. The total temperature rise was used to calculate the total charge. The zero-order polynomial fits were taken before the beam charging and after the temperature become stable when the tungsten is in the equilibrating position. The relationship between the total charge and the temperature rise is:

$$Charge = K * Temperature, \tag{1}$$

where $K$ is the heat capacity of tungsten. It was measured by Ahamad Mahmoud before the experiment [9]. The result is shown in Fig. 10 , with the value of $8555.5 \pm 50\, J/K$. $T$ is the average temperature from the 6 RTDs.

There are several devices needed to be calibrated, and each one has its own special condition. The detail calibration procedures for each device are as follows.

## 2.1 Calibration for SIS3800 scaler

A reset signal was sent to the SIS3800 scaler at the beginning of the run to clear the counts. Since the scaler was found to cause high deadtime, only clock signals were sampled for each event, while other signals were sampled for each 1000 events. Also the DAQ read the scaler once at the end of the run.

The middle left picture in Fig. 9 is for the SIS3800 calibration. The rise in the graph is the period when the beam hits the tungsten, corresponding to the rise in the top left. The total charge has the following relation with the counts:

$$Charge = slope * (\Delta counts - ped * \Delta clockcounts), \tag{2}$$

where $\Delta counts$ is the total BCM counts accumulated in the scaler, $\Delta clockcounts$ is the total clock counts accumulated in the scaler. The $ped$ is the pedestal value which is calculated from the first-order polynomial fits before and after the beam heats the tungsten. To get the $slope$ value, two time points are chosen before and after the beam. Using the $\Delta counts$ and the $\Delta clockcounts$ between these two time points and combining with the charge calculated from the temperature, the $slope$ value is then determined.

The beam current is calculated from the calibration constants as:

$$Current = slope * (rate - ped * clockrate), \tag{3}$$

where $rate$ and $clockrate$ are defined as the bcm counts per second and clock counts per second.

## 2.2 Calibration for SIS3801 scaler

To calibrate the SIS3801 scaler it is necessary to accumulate all of the counts for each helicity window, without any loss of data. There are two methods to get the total counts. One is using the sum counts from two virtual scalers. The offline analyzer [10] automatically accumulates the total counts for positive helicity state and negative helicity state, which present two independent variables (positive and negative virtual scaler) in the raw data. Another is accumulating all of the counts from the ringbuffer. The helicity decoder was used to check if data were lost. The calculated calibration constants are the same from the two methods. Further procedures are same as the SIS3800. The total charge has the following relation with the counts:

$$Charge = slope * (\Delta counts - ped * \Delta clockcounts), \tag{4}$$

where the $\Delta counts$ and $\Delta clockcounts$ are counted from the SIS3801 scaler. Since the SIS3801 does not count for 70 $\mu s$ for each 1041.65 $\mu s$, the slopes calculated for the SIS3801 are larger than the slope for the SIS3800. The beam current is calculated as:

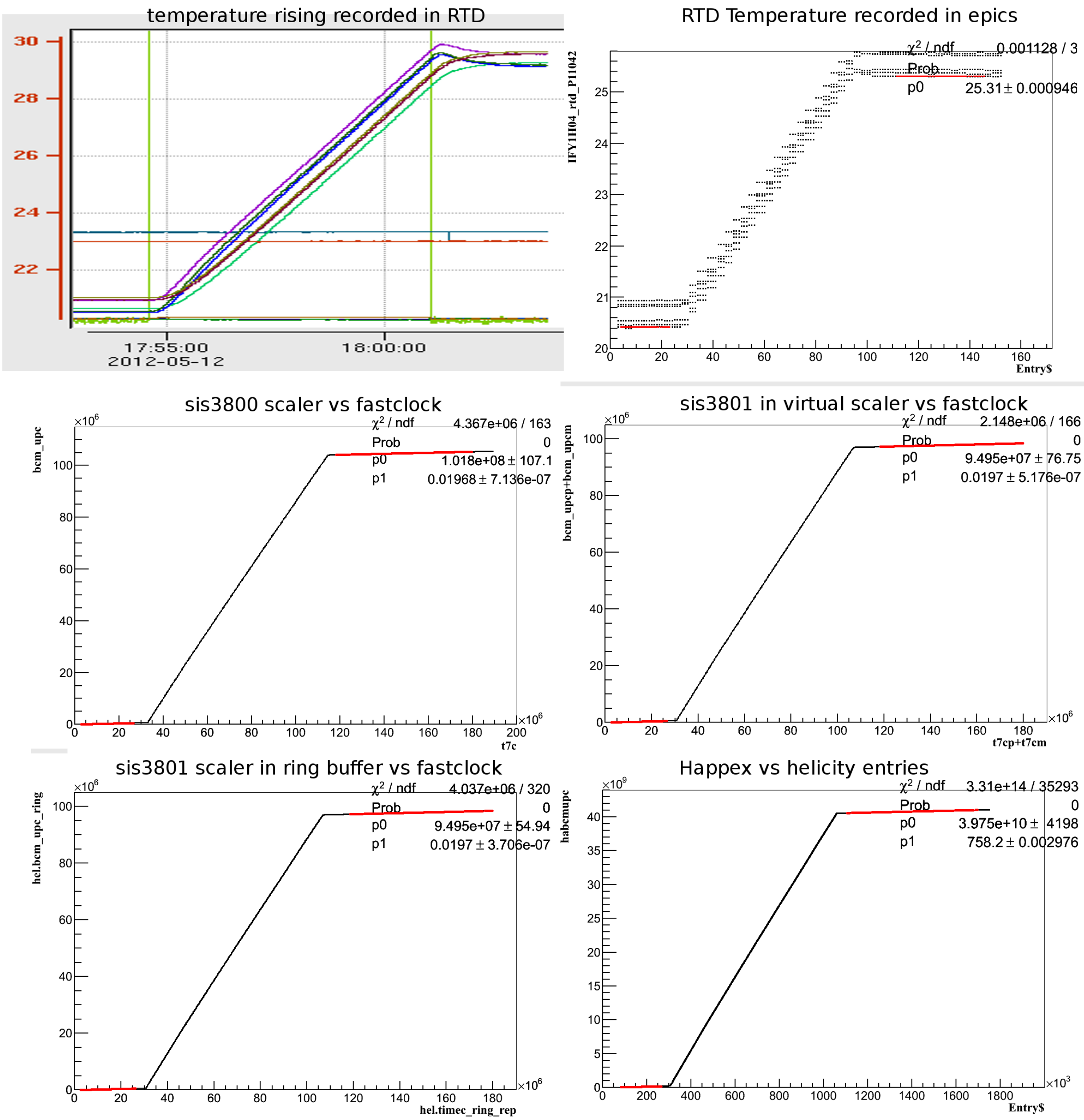


Figure 9: BCM Calibration, the top left and right figures are the temperature rise of the RTDs, the last four plots show the counts recorded in the scalers and the HAPPEX ADCs at the same time.

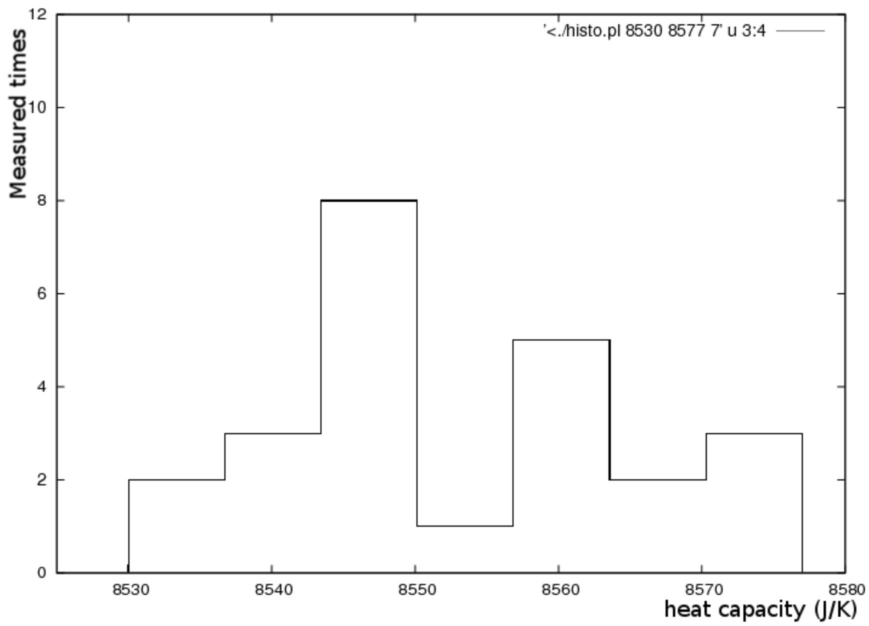


Figure 10: Tungsten Calorimeter Heat Capacity Determination [9]

$$Current = Slope * (rate - ped * 103700/s * 971.65\mu\text{s})/1041.65\mu s, \tag{5}$$

where $103700/s$ is the frequency of the fast clock, $971.65\mu$s is the duration of T-Stable, and $1041.65\mu s$ is the duration of a helicity window.

### 2.3 Calibration for HAPPEX ADC

To calibrate the HAPPEX ADC, the values are accumulated for all of the events between two time periods as the total counts. The entries in the HAPPEX DAQ are used as the time stamp. The total charge has the following relation with the counts:

$$Charge = slope * 875\mu\text{s} * (\Delta counts - ped * \Delta entries), \tag{6}$$

where $875\mu s$ is the integration time of the ADC. The beam current is calculated as:

$$Current = slope * (rate - ped) * 875\mu\text{s}/1041.65\mu\text{s}. \tag{7}$$

### 2.4 Uncertainty

The uncertainty of the calculated charge from the tungsten calorimeter comes from the beam energy, RTD, measured tungsten heat capacity, and the heat loss. The accuracy of the beam energy calculated from the ARC measurement [11] is 0.2 MeV in the range of 0.5 to 6 GeV [12], which contributes to the uncertainty of calculated charge of 0.34 nC per 1 K temperature rise (2.2 GeV beam energy). The uncertainties of the RTDs are 12.5 mK [13], which contributes uncertainty of $0.046\,\mu C$ (2.2 GeV beam energy). The $50\,J/K$ uncertainty of heat capacity contributes $0.18\,\mu C$ per 1 K temperature rise (2.2GeV beam energy). The Hall A calorimeter thermal and mechanical design limits heat losses to the $\sim$ 0.2% level if the measurement is within 20 minutes [7], which results in an uncertainty of the calculated charge of an additional 0.2 %. The total uncertainty is $\sim$ 0.68 % for the calculated charge from tungsten.

By comparing the difference between the upstream and downstream BCMs, the fluctuations between the two are below $0.19\,\mu C$ for 90% of runs. The relative differences between them for 90% runs are below 0.7%,

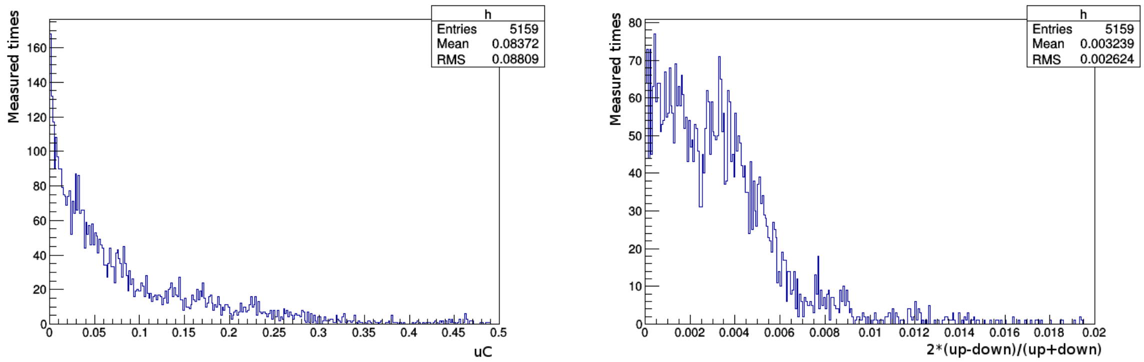


(a) Absolute difference between upstream and downstream charge

(b) Relative difference between upstream and downstream charge

Figure 11: Comparison of the charge calculated from the upstream and downstream BCMs. Each entry in the graph is the total charge calculated from each run from the experiment.

as shown in Fig. 11 . The differences indicate the uncertainty of the BCMs are below 0.7%. Combined with the uncertainty of the tungsten calorimeter, the final uncertainty of BCM is below 1%.

# 3 Calibration constants

The calibration constants are shown in the Appendix Tables 1-9. Some specials are listed below:

- begin - Mar.17 3rm downstream scaler abnormal
- Mar.18 - Apr.2 left arm upstream scaler noisy
- Apr.2 - Apr.9 right arm SIS3801 not working
- Apr.9 changed right arm scaler channel for bcm
- Apr.19 - calibration constant changed
- Near May.12 third arm SIS3801 not working
- May.13 - May.14 downstream bcm broken

The bcm receiver gain settings for each periods are list below, the values after the date are:
A_Pre_Gain_1/A_Pre_Gain_2/A_Mag_Div
B_Pre_Gain_1/B_Pre_Gain_2/B_Mag_Div
IQ_Filter_K
Mag_Filter_K

- begin - Mar.2 18:39:42 gain changing
- Mar.2 18:39:43 - Mar.5 10:00:12 10/10/1 9/9/1 3 4
- Mar.5 10:00:13 - Mar.5 10:27:40 gain changing
- Mar.5 10:27:41 - Mar.6 8:51:39 10/10/1 9/9/1 1 4
- Mar.6 8:51:40 - Mar.6 13:45:43 10/13/1 9/9/1 1 4
- Mar.6 13:45:44 - Mar.6 13:49:05 gain changing
- Mar.6 13:49:06 - Mar.7 17:20:10 29/30/4 27/27/4 1 4

- Mar.7 17:20:11 - Mar.7 17:23:25 gain changing
- Mar.7 17:23:25 - Mar.10 13:12:53 29/30/4 27/27/4 1 4
- Mar.10 13:12:54 - Mar.10 13:33:15 gain changing
- Mar.10 13:33:16 - end 40/41/4 40/43/4 1 4

# References


[1] J.-C. Denard, High Accuracy Beam Current Monitor System for CEBAF's Experimental Hall A, 2001 Particle Accelerator Conference, Chicago (2001) 2326 – 2328.

[2] J. Musson, Functional Description of Algorithms Used in Digital Receivers, JLab Technical Report No. JLAB-TN-14-028.

[3] S. H. Roger Flood, R. Suleiman, Helicity Control Board User's Guide, JLab Internal Manual (unpublished).
URL `http://hallaweb.jlab.org/equipment/daq/HelicityUsersGuideFeb4.pdf`

[4] Specification of HAPPEX II ADC Timing Board, Revision 1, JLab Technical Report (unpublished).
URL `http://hallaweb.jlab.org/experiment/g2p/technotes/others/TimingBoard.pdf`

[5] R. Michaels, Precision Integrating HAPPEX ADC, JLab Technical Report (unpublished).
URL `http://hallaweb.jlab.org/parity/prex/adc18/prex_adc18_spec.ps`

[6] E. Jastrzembski, A Flexible Vme Input/Output Module, JLab Technical Report (unpublished).
URL `https://coda.jlab.org/drupal/system/files/pdfs/HardwareManual/misc/FLEXIO.pdf`

[7] M. Bevins, A. Day, et al., Mechanical and Thermal Design of the CEBAF Hall A Beam Calorimeter, in: Proceedings of 2005 Particle Accelerator Conference, 2005, pp. 3819–3821. doi:10.1109/PAC.2005.1591634.

[8] Pengjia Zhu, et al, Beam Position Reconstruction for the g2p Experiment in Hall A at Jefferson Lab, Nuclear Instruments and Methods in Physics Research Section A: Accelerators, Spectrometers, Detectors and Associated Equipment 808 (2016) 1 – 10. doi:http://dx.doi.org/10.1016/j.nima.2015.10.086.
URL `http://www.sciencedirect.com/science/article/pii/S0168900215013200`

[9] G2P Internal Elog, https://hallaweb.jlab.org/dvcslog/g2p/173.

[10] O. Hansen, ROOT/C++ Analyzer for Hall A.
URL `http://hallaweb.jlab.org/podd/index.html`

[11] J. Alcorn, et al., Basic instrumentation for hall a at jefferson lab, Nuclear Instruments and Methods in Physics Research Section A: Accelerators, Spectrometers, Detectors and Associated Equipment 522 (3) (2004) 294 – 346. doi:http://dx.doi.org/10.1016/j.nima.2003.11.415.
URL `http://www.sciencedirect.com/science/article/pii/S0168900203033977`

[12] JLab webpage, http://hallaweb.jlab.org/equipment/beam/absol_beam.html.

[13] Y. Rousseau, Calibration of the Calorimeter, JLab Technical Report (unpublished).
URL `http://hallaweb.jlab.org/experiment/g2p/technotes/others/calorimeter%20RTD.pdf`


# Appendix

| current(nA) | 280 | 25 | 50 | 75 | 100 |
|---|---|---|---|---|---|
| energy(MeV) | 2253.13 | 2252.94 | 2252.94 | 2252.94 | 2252.94 |
| time | 03/03/12 09:30 PM | 03/13/12 04:00 PM | 03/16/12 10:15 PM | 03/29/12 12:21 AM | 04/07/12 03:00 PM |
| Avail period | Start 3.10 13:25 | 3.10 13:33 3.17 10:00 | 3.10 13:33 3.17 10:00 | 3.27 21:00 4.2 14:00 | 4.2 18:00 4.9 9:00 |
| run avail(left SIS3800 up) | Start 3051 | 3052 3295 | 3052 3295 | broken | 3660 4695 |
| run avail(left SIS3800 down) | Start 3051 | 3052 3634 | 3052 3634 | 3052 3634 | 3636 4695 |
| run avail(left SIS3801 up) | Start 3051 | 3052 3295 | 3052 3295 | broken | 3660 4695 |
| run avail(left SIS3801 down) | Start 3051 | 3052 3634 | 3052 3634 | 3052 3634 | 3636 4695 |
| run avail(left HAPPEX up) | Start 3051 | | | 3073 3634 | 3636 4695 |
| run avail(left HAPPEX down) | Start 3051 | | | 3073 3634 | 3636 4695 |
| runnumber | 2665 | 3149 | 3254 | 3437 | 3856 |
| SIS3800 upslope(slowclk) | 1.37309e-06 | 3.32775e-07 | 3.34603E-07 | 2.30692e-07 | 3.22991E-07 |
| SIS3800 upped(slowclk) | 5.24344E+00 | 2.04717E+00 | 2.01363E+00 | 2.40785E+00 | 2.01757E+00 |
| SIS3800 downslope(slowclk) | 1.30711e-06 | 2.58036e-07 | 2.57738E-07 | 2.56379e-07 | 2.49656E-07 |
| SIS3800 downped(slowclk) | 6.91734E+00 | 2.76818E+00 | 2.73600E+00 | 2.58978E+00 | 2.73382E+00 |
| SIS3800 upslope(fstclk) | 1.37346e-06 | 3.32774e-07 | 3.34604E-07 | 2.30693e-07 | 3.22990E-07 |
| SIS3800 upped(fstclk) | 5.17426E-02 | 2.01725E-02 | 1.98515E-02 | 2.37558E-02 | 1.98845E-02 |
| SIS3800 downslope(fstclk) | 1.30736e-06 | 2.58035e-07 | 2.57739E-07 | 2.5638e-07 | 2.49655E-07 |
| SIS3800 downped(fstclk) | 6.82245E-02 | 2.72772E-02 | 2.69731E-02 | 2.55486E-02 | 2.69437E-02 |
| SIS3801 upslope(fstclk) | 1.47161e-06 | 3.65962e-07 | 3.58951e-07 | 2.4832e-07 | 3.46231e-07 |
| SIS3801 upped(fstclk) | 5.15461E-02 | 3.09438E-02 | 1.98588E-02 | 2.37232E-02 | 1.98880E-02 |
| SIS3801 downslope(fstclk) | 1.40127e-06 | 2.83756e-07 | 2.76493e-07 | 2.7518e-07 | 2.67616e-07 |
| SIS3801 downped(fstclk) | 6.81238E-02 | 4.11454E-02 | 2.69735E-02 | 2.55914E-02 | 2.69484E-02 |
| HAPPEX upslope | not avail | | | 9.76018e-07 | 9.44277E-07 |
| HAPPEX upped | not avail | | | 7.47561E+02 | 7.64707E+02 |
| HAPPEX downslope | not avail | | | 7.81678e-07 | 7.59977E-07 |
| HAPPEX downped | not avail | | | 7.06877E+02 | 7.27266E+02 |

Table 1: BCM calibration constants for the left arm

| current(nA) | 50 | 75 | 50 | 25 | 50 |
|---|---|---|---|---|---|
| energy(MeV) | 1712.19 | 1708.35 | 1156.7 | 1156.7 | 2253.65 |
| time | 04/10/12 08:09 AM | 04/14/12 07:07 PM | 04/25/12 02:38 AM | 04/28/12 10:15 AM | 05/06/12 02:43 PM |
| Avail period | 4.10 0:00 4.19 8:00 | 4.10 0:00 4.19 8:00 | 4.20 4:00 5.2 8:00 | 4.20 4:00 5.2 8:00 | 5.2 21:00 5.13 1:00 |
| run avail(left SIS3800 up) | 3660 4695 | 3660 4695 | 4698 5440 | 4698 5440 | 5485 6100 |
| run avail(left SIS3800 down) | 3636 4695 | 3636 4695 | 4698 5440 | 4698 5440 | 5485 6043 |
| run avail(left SIS3801 up) | 3660 4695 | 3660 4695 | 4698 5440 | 4698 5440 | 5485 6100 |
| run avail(left SIS3801 down) | 3636 4695 | 3636 4695 | 4698 5440 | 4698 5440 | 5485 6043 |
| run avail(left HAPPEX up) | | | 4698 5440 | 4698 5440 | 5485 6100 |
| run avail(left HAPPEX down) | | | 4698 5440 | 4698 5440 | 5485 6043 |
| runnumber | 4088 | 4405 | 5015 | 5214 | 5751 |
| SIS3800 upslope(slowclk) | 3.19668E-07 | 3.23814E-07 | 3.55483E-07 | 3.53225E-07 | 3.48943E-07 |
| SIS3800 upped(slowclk) | 2.02148E+00 | 2.02217E+00 | 1.99755E+00 | 2.03317E+00 | 2.00619E+00 |
| SIS3800 downslope(slowclk) | 2.47684E-07 | 2.48227E-07 | 2.58163E-07 | 2.57395E-07 | 2.54841E-07 |
| SIS3800 downped(slowclk) | 2.73704E+00 | 2.74181E+00 | 2.71992E+00 | 2.75600E+00 | 2.74454E+00 |
| SIS3800 upslope(fstclk) | 3.19669E-07 | 3.23815E-07 | 3.55483E-07 | 3.53221E-07 | 3.48942E-07 |
| SIS3800 upped(fstclk) | 1.99247E-02 | 1.99301E-02 | 1.96837E-02 | 2.00331E-02 | 1.97694E-02 |
| SIS3800 downslope(fstclk) | 2.47685E-07 | 2.48228E-07 | 2.58163E-07 | 2.57392E-07 | 2.54841E-07 |
| SIS3800 downped(fstclk) | 2.69776E-02 | 2.70227E-02 | 2.68033E-02 | 2.71552E-02 | 2.70453E-02 |
| SIS3801 upslope(fstclk) | 3.42781e-07 | 3.4717e-07 | 3.81166e-07 | 3.78808e-07 | 3.7418e-07 |
| SIS3801 upped(fstclk) | 1.99254E-02 | 1.99350E-02 | 1.97021E-02 | 2.00361E-02 | 1.97749E-02 |
| SIS3801 downslope(fstclk) | 2.65591e-07 | 2.6613e-07 | 2.76814e-07 | 2.76033e-07 | 2.73271e-07 |
| SIS3801 downped(fstclk) | 2.69789E-02 | 2.70306E-02 | 2.68191E-02 | 2.71594E-02 | 2.70443E-02 |
| HAPPEX upslope | | | 1.04042E-06 | 1.03394E-06 | 1.02106E-06 |
| HAPPEX upped | | | 7.58219E+02 | 7.74628E+02 | 7.63704E+02 |
| HAPPEX downslope | | | 7.86150E-07 | 7.84135E-07 | 7.76177E-07 |
| HAPPEX downped | | | 7.25062E+02 | 7.39477E+02 | 7.35583E+02 |

Table 2: BCM calibration constants for the left arm

| current(nA) | 75 | 100 | 50 | 75 |
|---|---|---|---|---|
| energy(MeV) | 2253.34 | 2253.37 | 2252.94 | 3352.4 |
| time | 05/11/12 06:26 PM | 05/12/12 05:48 PM | 05/13/12 02:59 PM | 05/16/12 11:41 PM |
| Avail period | 5.2 21:00 5.13 1:00 | 5.2 21:00 5.13 1:00 | 5.13 1:00 5.14 8:00 | 5.14 15:00 end |
| run avail(left SIS3800 up) | 5485 6100 | 5485 6100 | 5485 6100 | 6101 end |
| run avail(left SIS3800 down) | 5485 6043 | 5485 6043 | broken | 6101 end(NR) |
| run avail(left SIS3801 up) | 5485 6100 | 5485 6100 | 5485 6100 | 6101 end |
| run avail(left SIS3801 down) | 5485 6043 | 5485 6043 | broken | 6101 end(NR) |
| run avail(left HAPPEX up) | 5485 6100 | 5485 6100 | 5485 6100 | 6101 end |
| run avail(left HAPPEX down) | 5485 6043 | 5485 6043 | broken | 6101 end(NR) |
| runnumber | 5986 | 6035 | 6062 | 6174 |
| SIS3800 upslope(slowclk) | 3.49032E-07 | 3.47590E-07 | 3.50492E-07 | 3.55051e-07 |
| SIS3800 upped(slowclk) | 2.01442E+00 | 2.01317E+00 | 2.01224E+00 | 2.00844E+00 |
| SIS3800 downslope(slowclk) | 2.54925E-07 | 2.53945E-07 | 1.96575E-06 | 2.57619e-07 |
| SIS3800 downped(slowclk) | 2.72054E+00 | 2.71869E+00 | 2.71795E+00 | 2.73275E+00 |
| SIS3800 upslope(fstclk) | 3.49036E-07 | 3.47589E-07 | 3.50490E-07 | 3.55056e-07 |
| SIS3800 upped(fstclk) | 1.98566E-02 | 1.98398E-02 | 1.98255E-02 | 1.97970E-02 |
| SIS3800 downslope(fstclk) | 2.54928E-07 | 2.53944E-07 | 1.96567E-06 | 2.57623e-07 |
| SIS3800 downped(fstclk) | 2.68156E-02 | 2.67923E-02 | 2.67783E-02 | 2.69365E-02 |
| SIS3801 upslope(fstclk) | 3.74239e-07 | 3.72691e-07 | 3.75909e-07 | 3.80653e-07 |
| SIS3801 upped(fstclk) | 1.98584E-02 | 1.98459E-02 | 1.98381E-02 | 1.97998E-02 |
| SIS3801 downslope(fstclk) | 2.73332e-07 | 2.72283e-07 | 2.10829e-06 | 2.76198e-07 |
| SIS3801 downped(fstclk) | 2.68168E-02 | 2.67972E-02 | 2.68024E-02 | 2.69430E-02 |
| HAPPEX upslope | 1.02102E-06 | 1.01675E-06 | 1.02575E-06 | 1.03841e-06 |
| HAPPEX upped | 7.66377E+02 | 7.66642E+02 | 7.65561E+02 | 7.60940E+02 |
| HAPPEX downslope | 7.76257E-07 | 7.73150E-07 | 5.97952E-06 | 7.84284e-07 |
| HAPPEX downped | 7.26879E+02 | 7.26759E+02 | 7.23959E+02 | 7.29082E+02 |

Table 3: BCM calibration constants for the left arm

| current(nA) | 280 | 25 | 50 | 75 | 100 |
|---|---|---|---|---|---|
| energy(MeV) | 2253.13 | 2252.94 | 2252.94 | 2252.94 | 2252.94 |
| time | 03/03/12 09:30 PM | 03/13/12 04:00 PM | 03/16/12 10:15 PM | 03/29/12 12:21 AM | 04/07/12 03:00 PM |
| Avail period | Start 3.10 13:25 | 3.10 13:33 3.17 10:00 | 3.10 13:33 3.17 10:00 | 3.27 21:00 4.2 14:00 | 4.2 18:00 4.9 9:00 |
| run avail(right SIS3800 up) | Start 22130 | 22131 22658 | 22131 22658 | 22131 22658 | 22660 22987 |
| run avail(right SIS3800 down) | Start 22130 | 22131 22658 | 22131 22658 | 22131 22658 | 22660 22987 |
| run avail(right SIS3801 up) | Start 22130 | 22131 22658 | 22131 22658 | 22131 22658 | broken |
| run avail(right SIS3801 down) | Start 22130 | 22131 22658 | 22131 22658 | 22131 22658 | broken |
| run avail(right HAPPEX up) | Start 22130 | | | 22158 22658 | 22660 23618 |
| run avail(right HAPPEX down) | Start 22130 | | | 22158 22658 | 22660 23618 |
| runnumber | 21751 | 22238 | 22338 | 22470 | 22885 |
| SIS3800 upslope(slowclk) | 1.37212e-06 | 3.33141E-07 | 3.35299E-07 | 3.33446E-07 | 3.22819E-07 |
| SIS3800 upped(slowclk) | 5.23480E+00 | 2.04715E+00 | 2.01363E+00 | 1.88817E+00 | 2.01757E+00 |
| SIS3800 downslope(slowclk) | 1.30632e-06 | 2.58320E-07 | 2.58274E-07 | 2.56520E-07 | 2.49523E-07 |
| SIS3800 downped(slowclk) | 6.91143E+00 | 2.76815E+00 | 2.73599E+00 | 2.58975E+00 | 2.73382E+00 |
| SIS3800 upslope(fstclk) | 1.37253e-06 | 3.33139E-07 | 3.35301E-07 | 3.33445E-07 | 3.22818E-07 |
| SIS3800 upped(fstclk) | 5.16652E-02 | 2.01720E-02 | 1.98516E-02 | 1.86263E-02 | 1.98844E-02 |
| SIS3800 downslope(fstclk) | 1.30656e-06 | 2.58318E-07 | 2.58276E-07 | 2.56521E-07 | 2.49521E-07 |
| SIS3800 downped(fstclk) | 6.81632E-02 | 2.72768E-02 | 2.69733E-02 | 2.55485E-02 | 2.69437E-02 |
| SIS3801 upslope(fstclk) | 1.46934e-06 | 3.65342e-07 | 3.59699e-07 | 3.57709e-07 | broken |
| SIS3801 upped(fstclk) | 5.16033E-02 | 2.97348E-02 | 1.98585E-02 | 1.86580E-02 | broken |
| SIS3801 downslope(fstclk) | 1.39902e-06 | 2.83277e-07 | 2.77067e-07 | 2.75175e-07 | broken |
| SIS3801 downped(fstclk) | 6.81575E-02 | 3.95893E-02 | 2.69721E-02 | 2.55542E-02 | broken |
| HAPPEX upslope | not avail | | | 9.55044e-07 | 9.23204E-07 |
| HAPPEX upped | not avail | | | 1.75740E+03 | 1.75756E+03 |
| HAPPEX downslope | not avail | | | 7.81495e-07 | 7.59968E-07 |
| HAPPEX downped | not avail | | | 1.07545E+03 | 1.07213E+03 |

Table 4: BCM calibration constants for the right arm

| current(nA) | 50 | 75 | 50 | 25 | 50 |
|---|---|---|---|---|---|
| energy(MeV) | 1712.19 | 1708.35 | 1156.7 | 1156.7 | 2253.65 |
| time | 04/10/12 08:09 AM | 04/14/12 07:07 PM | 04/25/12 02:38 AM | 04/28/12 10:15 AM | 05/06/12 02:43 PM |
| Avail period | 4.10 0:00 4.19 8:00 | 4.10 0:00 4.19 8:00 | 4.20 4:00 5.2 8:00 | 4.20 4:00 5.2 8:00 | 5.2 21:00 5.13 1:00 |
| run avail(right SIS3800 up) | 22600 23618 | 22600 23618 | 23621 24216 | 23621 24216 | 24259 24727 |
| run avail(right SIS3800 down) | 22600 23618 | 22600 23618 | 23621 24216 | 23621 24216 | 24259 24706 |
| run avail(right SIS3801 up) | 23075 23618 | 23075 23618 | 23621 24216 | 23621 24216 | 24259 24727 |
| run avail(right SIS3801 down) | 23075 23618 | 23075 23618 | 23621 24216 | 23621 24216 | 24259 24706 |
| run avail(right HAPPEX up) | | | 23621 24216 | 23621 24216 | 24259 24727 |
| run avail(right HAPPEX down) | | | 23621 24216 | 23621 24216 | 24259 24706 |
| runnumber | 23082 | 23360 | 23890 | 24040 | 24458 |
| SIS3800 upslope(slowclk) | 3.19449E-07 | 3.23652E-07 | 3.55750E-07 | 3.53327E-07 | 3.48757E-07 |
| SIS3800 upped(slowclk) | 2.02144E+00 | 2.02219E+00 | 1.99750E+00 | 2.03317E+00 | 2.00620E+00 |
| SIS3800 downslope(slowclk) | 2.47514E-07 | 2.48103E-07 | 2.58357E-07 | 2.57469E-07 | 2.54705E-07 |
| SIS3800 downped(slowclk) | 2.73699E+00 | 2.74179E+00 | 2.71988E+00 | 2.75600E+00 | 2.74454E+00 |
| SIS3800 upslope(fstclk) | 3.19451E-07 | 3.23653E-07 | 3.55750E-07 | 3.53323E-07 | 3.48756E-07 |
| SIS3800 upped(fstclk) | 1.99248E-02 | 1.99306E-02 | 1.96839E-02 | 2.00331E-02 | 1.97694E-02 |
| SIS3800 downslope(fstclk) | 2.47516E-07 | 2.48103E-07 | 2.58357E-07 | 2.57466E-07 | 2.54705E-07 |
| SIS3800 downped(fstclk) | 2.69778E-02 | 2.70229E-02 | 2.68034E-02 | 2.71552E-02 | 2.70453E-02 |
| SIS3801 upslope(fstclk) | 3.42548e-07 | 3.46997e-07 | 3.81454e-07 | 3.78918e-07 | 3.7398e-07 |
| SIS3801 upped(fstclk) | 1.99254E-02 | 1.99350E-02 | 1.97020E-02 | 2.00361E-02 | 1.97749E-02 |
| SIS3801 downslope(fstclk) | 2.6541e-07 | 2.65997e-07 | 2.77022e-07 | 2.76114e-07 | 2.73125e-07 |
| SIS3801 downped(fstclk) | 2.69789E-02 | 2.70307E-02 | 2.68188E-02 | 2.71595E-02 | 2.70442E-02 |
| HAPPEX upslope | | | 1.01836E-06 | 1.01194E-06 | 9.98575E-07 |
| HAPPEX upped | | | 1.76323E+03 | 1.77658E+03 | 1.76456E+03 |
| HAPPEX downslope | | | 7.86595E-07 | 7.84236E-07 | 7.75621E-07 |
| HAPPEX downped | | | 1.09454E+03 | 1.10431E+03 | 1.10078E+03 |

Table 5: BCM calibration constants for the right arm

| current(nA) | 75 | 100 | 50 | 75 |
|---|---|---|---|---|
| energy(MeV) | 2253.34 | 2253.37 | 2252.94 | 3352.4 |
| time | 05/11/12 06:26 PM | 05/12/12 05:48 PM | 05/13/12 02:59 PM | 05/16/12 11:41 PM |
| Avail period | 5.2 21:00 5.13 1:00 | 5.2 21:00 5.13 1:00 | 5.13 1:00 5.14 8:00 | 5.14 15:00 end |
| run avail(right SIS3800 up) | 24259 24727 | 24259 24727 | 24259 24727 | 24728 end |
| run avail(right SIS3800 down) | 24259 24706 | 24259 24706 | broken | 24728 end(NR) |
| run avail(right SIS3801 up) | 24259 24727 | 24259 24727 | 24259 24727 | 24728 end |
| run avail(right SIS3801 down) | 24259 24706 | 24259 24706 | broken | 24728 end(NR) |
| run avail(right HAPPEX up) | 24259 24727 | 24259 24727 | 24259 24727 | 24728 end |
| run avail(right HAPPEX down) | 24259 24706 | 24259 24706 | broken | 24728 end(NR) |
| runnumber | 24671 | 24700 | 24719 | 24769 |
| SIS3800 upslope(slowclk) | 3.49296E-07 | 3.47708E-07 | 3.50342E-07 | 3.54078E-07 |
| SIS3800 upped(slowclk) | 2.01441E+00 | 2.01317E+00 | 2.01224E+00 | 2.00686E+00 |
| SIS3800 downslope(slowclk) | 2.55118E-07 | 2.54031E-07 | 1.96491E-06 | 2.56913E-07 |
| SIS3800 downped(slowclk) | 2.72053E+00 | 2.71870E+00 | 2.71795E+00 | 2.73056E+00 |
| SIS3800 upslope(fstclk) | 3.49301E-07 | 3.47708E-07 | 3.50340E-07 | 3.54078E-07 |
| SIS3800 upped(fstclk) | 1.98572E-02 | 1.98398E-02 | 1.98256E-02 | 1.97767E-02 |
| SIS3800 downslope(fstclk) | 2.55121E-07 | 2.54031E-07 | 1.96483E-06 | 2.56913E-07 |
| SIS3800 downped(fstclk) | 2.68159E-02 | 2.67923E-02 | 2.67784E-02 | 2.69082E-02 |
| SIS3801 upslope(fstclk) | 3.74523e-07 | 3.72818e-07 | 3.75748e-07 | 3.79606e-07 |
| SIS3801 upped(fstclk) | 1.98591E-02 | 1.98461E-02 | 1.98382E-02 | 1.97795E-02 |
| SIS3801 downslope(fstclk) | 2.7354e-07 | 2.72376e-07 | 2.10737e-06 | 2.75437e-07 |
| SIS3801 downped(fstclk) | 2.68172E-02 | 2.67970E-02 | 2.68023E-02 | 2.69125E-02 |
| HAPPEX upslope | 9.99842E-07 | 9.95083E-07 | 1.00323E-06 | 1.01328E-06 |
| HAPPEX upped | 1.77152E+03 | 1.77303E+03 | 1.77264E+03 | 1.76628E+03 |
| HAPPEX downslope | 7.76667E-07 | 7.73271E-07 | 5.97638E-06 | 7.82040E-07 |
| HAPPEX downped | 1.08914E+03 | 1.08845E+03 | 1.08867E+03 | 1.09584E+03 |

Table 6: BCM calibration constants for the right arm

| current(nA) | 280 | 25 | 50 | 75 | 100 |
|---|---|---|---|---|---|
| energy(MeV) | 2253.13 | 2252.94 | 2252.94 | 2252.94 | 2252.94 |
| time | 03/03/12 09:30 PM | 03/13/12 04:00 PM | 03/16/12 10:15 PM | 03/29/12 12:21 AM | 04/07/12 03:00 PM |
| Avail period | Start 3.10 13:25 | 3.10 13:33 3.17 10:00 | 3.10 13:33 3.17 10:00 | 3.27 21:00 4.2 14:00 | 4.2 18:00 4.9 9:00 |
| run avail(third SIS3800 up) | not avail | 40296 40668 | 40296 40668 | 40296 40668 | 40670 41419 |
| run avail(third SIS3800 down) | not avail | broken | broken | 40465 40668 | 40670 41419 |
| run avail(third SIS3801 up) | not avail | 40296 40668 | 40296 40668 | 40296 40668 | 40670 41419 |
| run avail(third SIS3801 down) | not avail | broken | broken | 40465 40668 | 40670 41419 |
| runnumber | | 40368 | 40388 | 40486 | 40928 |
| SIS3800 upslope(fstclk) | not avail | 3.32885e-07 | 3.34957E-07 | 3.36286e-07 | 3.23371E-07 |
| SIS3800 upped(fstclk) | not avail | 2.01732E-02 | 1.98517E-02 | 1.98266E-02 | 1.98850E-02 |
| SIS3800 downslope(fstclk) | not avail | 1.2906e-07 | 1.29005E-07 | 2.5868e-07 | 2.49949E-07 |
| SIS3800 downped(fstclk) | not avail | 5.45561E-02 | 5.39468E-02 | 2.68700E-02 | 2.69434E-02 |
| SIS3801 upslope(fstclk) | not avail | 3.57236e-07 | 3.59326e-07 | 3.60744e-07 | 3.46631e-07 |
| SIS3801 upped(fstclk) | not avail | 2.02169E-02 | 1.98582E-02 | 1.98876E-02 | 1.98876E-02 |
| SIS3801 downslope(fstclk) | not avail | 1.38495e-07 | 1.38383e-07 | 2.77492e-07 | 2.67924e-07 |
| SIS3801 downped(fstclk) | not avail | 5.46740E-02 | 5.39542E-02 | 2.69487E-02 | 2.69487E-02 |

Table 7: BCM calibration constants for the third arm

| current(nA) | 50 | 75 | 50 | 25 | 50 |
|---|---|---|---|---|---|
| energy(MeV) | 1712.19 | 1708.35 | 1156.7 | 1156.7 | 2253.65 |
| time | 04/10/12 08:09 AM | 04/14/12 07:07 PM | 04/25/12 02:38 AM | 04/28/12 10:15 AM | 05/06/12 02:43 PM |
| Avail period | 4.10 0:00 4.19 8:00 | 4.10 0:00 4.19 8:00 | 4.20 4:00 5.2 8:00 | 4.20 4:00 5.2 8:00 | 5.2 21:00 5.13 1:00 |
| run avail(third SIS3800 up) | 40670 41419 | 40670 41419 | 41420 41915 | 41420 41915 | 41922 42052 |
| run avail(third SIS3800 down) | 40670 41419 | 40670 41419 | 41420 41915 | 41420 41915 | 41922 42017 |
| run avail(third SIS3801 up) | 40670 41419 | 40670 41419 | 41420 41915 | 41420 41915 | 41922 42052 |
| run avail(third SIS3801 down) | 40670 41419 | 40670 41419 | 41420 41915 | 41420 41915 | 41922 42017 |
| runnumber | 41027 | 41256 | 41671 | 41846 | 41918 |
| SIS3800 upslope(fstclk) | 3.19302E-07 | 3.23944E-07 | 3.56080E-07 | 3.53600E-07 | 3.48498E-07 |
| SIS3800 upped(fstclk) | 1.99247E-02 | 1.99308E-02 | 1.96874E-02 | 2.00331E-02 | 1.97662E-02 |
| SIS3800 downslope(fstclk) | 2.47400E-07 | 2.48326E-07 | 2.58596E-07 | 2.57668E-07 | 2.54516E-07 |
| SIS3800 downped(fstclk) | 2.69776E-02 | 2.70230E-02 | 2.68065E-02 | 2.71551E-02 | 2.70411E-02 |
| SIS3801 upslope(fstclk) | 3.46631e-07 | 3.47304e-07 | 3.81801e-07 | 3.79211e-07 | 3.73698e-07 |
| SIS3801 upped(fstclk) | 1.98876E-02 | 1.99356E-02 | 1.97044E-02 | 2.00362E-02 | 1.97719E-02 |
| SIS3801 downslope(fstclk) | 2.67924e-07 | 2.66232e-07 | 2.77274e-07 | 2.76326e-07 | 2.72918e-07 |
| SIS3801 downped(fstclk) | 2.69487E-02 | 2.70302E-02 | 2.68213E-02 | 2.71590E-02 | 2.70400E-02 |

Table 8: BCM calibration constants for the third arm

| current(nA) | 75 | 100 | 50 | 75 |
|---|---|---|---|---|
| energy(MeV) | 2253.34 | 2253.37 | 2252.94 | 3352.4 |
| time | 05/11/12 06:26 PM | 05/12/12 05:48 PM | 05/13/12 02:59 PM | 05/16/12 11:41 PM |
| Avail period | 5.2 21:00 5.13 1:00 | 5.2 21:00 5.13 1:00 | 5.13 1:00 5.14 8:00 | 5.14 15:00 end |
| run avail(third SIS3800 up) | 41922 42052 | 41922 42052 | 41922 42052 | 42053 end |
| run avail(third SIS3800 down) | 41922 42017 | 41922 42017 | broken | 42053 end(NR) |
| run avail(third SIS3801 up) | 41922 42052 | not avail | 41922 42052 | 42053 end |
| run avail(third SIS3801 down) | 41922 42017 | not avail | broken | 42053 end(NR) |
| runnumber | 41968 | 42008 | 42036 | 42126 |
| SIS3800 upslope(fstclk) | 3.49381E-07 | 3.47768E-07 | 3.50458E-07 | 3.54554E-07 |
| SIS3800 upped(fstclk) | 1.98550E-02 | 1.98381E-02 | 1.98268E-02 | 1.97758E-02 |
| SIS3800 downslope(fstclk) | 2.55180E-07 | 2.54075E-07 | 1.96554E-06 | 2.57258E-07 |
| SIS3800 downped(fstclk) | 2.68130E-02 | 2.67914E-02 | 2.67804E-02 | 2.69069E-02 |
| SIS3801 upslope(fstclk) | 3.74607e-07 | not avail | 3.75868e-07 | 3.80113e-07 |
| SIS3801 upped(fstclk) | 1.98589E-02 | not avail | 1.98389E-02 | 1.97786E-02 |
| SIS3801 downslope(fstclk) | 2.736e-07 | not avail | 2.10805e-06 | 2.75803e-07 |
| SIS3801 downped(fstclk) | 2.68173E-02 | not avail | 2.68024E-02 | 2.69116E-02 |

Table 9: BCM calibration constants for the third arm